

Bottomonium suppression and elliptic flow in heavy-ion collisions

Michael Strickland

Kent State University
Kent, OH USA

N. Brambilla, M.-A. Escobedo, MS, A. Vairo, P. Vander Griend,
and J.H. Weber, 2012.01240 and 2107.06222

H. Ba Omar, M. Escobedo, A. Islam, MS, S. Thapa, P. Vander Griend,
and J. Weber, 2107.06147 (open-source Qtraj 1.0 code release)

Hadrons 2021

19th International Conference on Hadron Spectroscopy and Structure

Mexico City; July 26-31, 2021



U.S. DEPARTMENT OF
ENERGY



Ohio Supercomputer Center
An OH·TECH Consortium Member

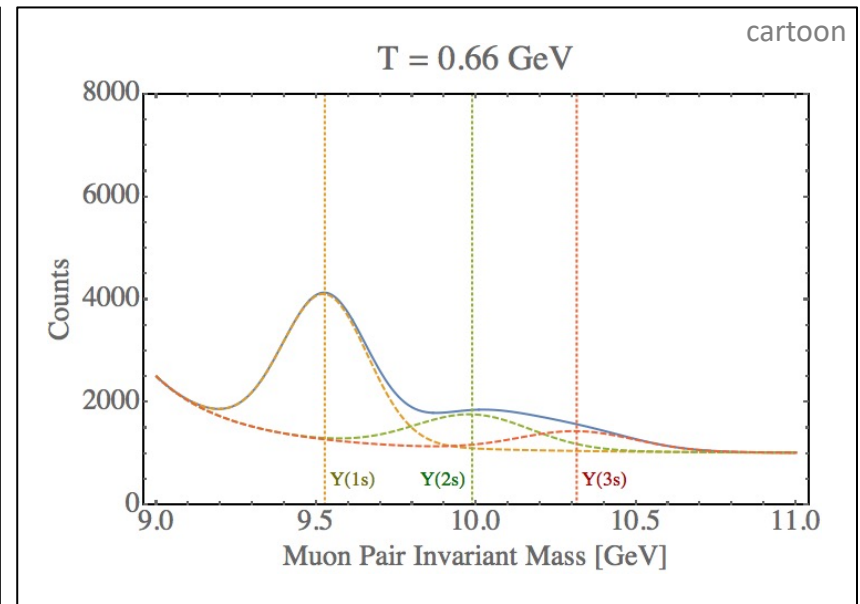
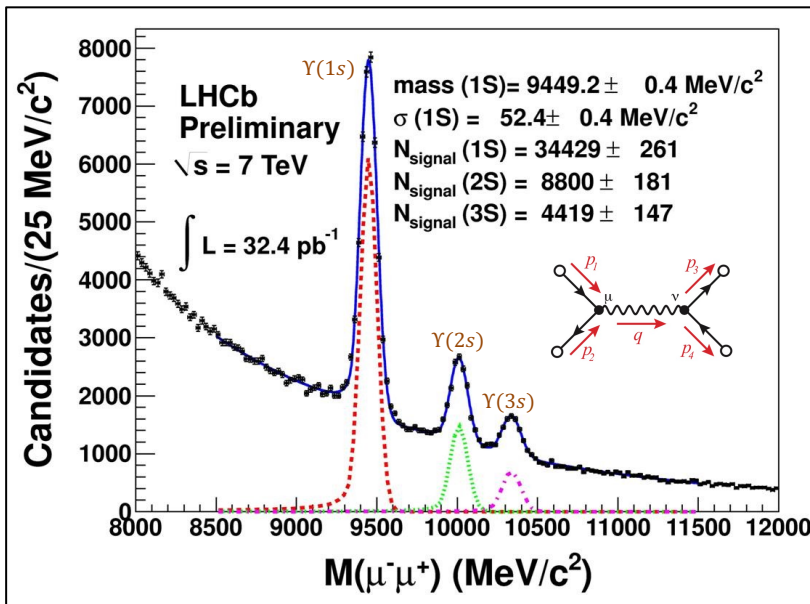
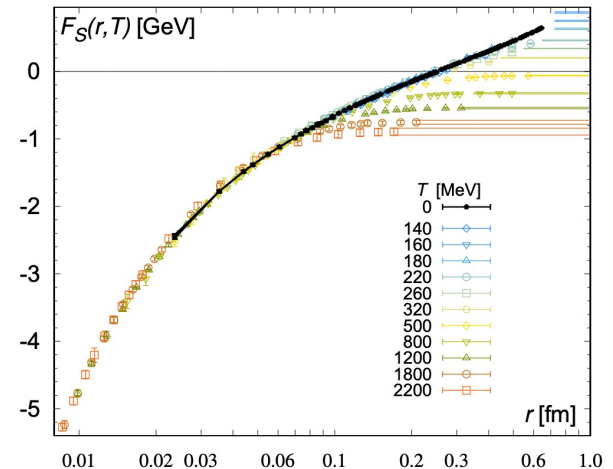
Bottomonium Suppression

- In a high temperature quark-gluon plasma we expect **weaker color binding** (Debye screening + asymptotic freedom)

E. V. Shuryak, Phys. Rept. 61, 71–158 (1980)
 T. Matsui, and H. Satz, Phys. Lett. B178, 416 (1986)
 F. Karsch, M. T. Mehr, and H. Satz, Z. Phys. C37, 617 (1988)

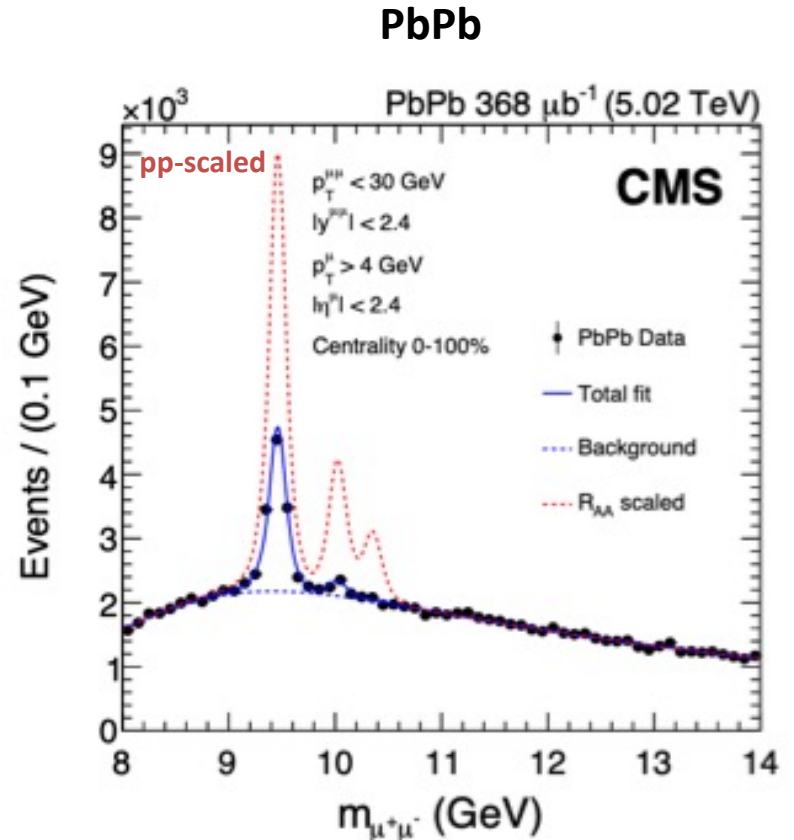
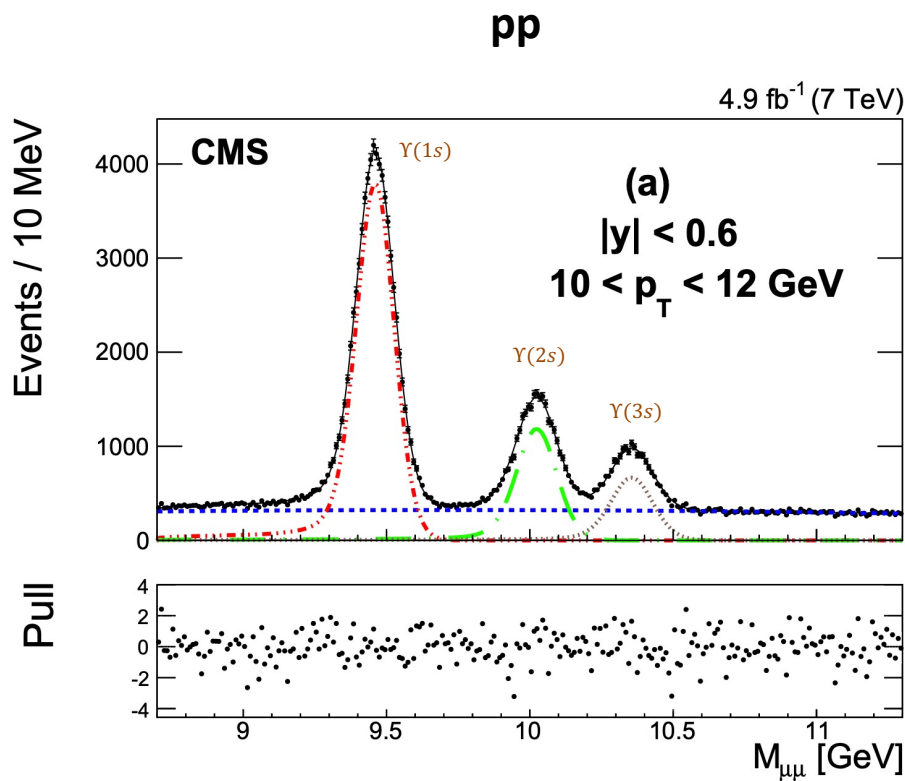
- Also, high energy plasma particles which slam into the bound states cause them to have shorter lifetimes → **larger spectral widths**

TUMQCD Collaboration, 1804.10600

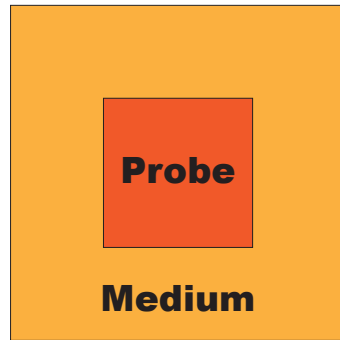


Experimental data – 5.02 TeV Dimuon Spectra

The **CMS**, **ALICE**, and **ATLAS** experiments have measured bottomonium production in both pp and Pb-Pb collisions. Here I show CMS results.



Open quantum system (OQS) approach



Probe = heavy-quarkonium state

Medium = light quarks and gluons that comprise the QGP

- Can treat heavy quarkonium states propagating through QGP using an open quantum system approach

$$H_{\text{tot}} = H_{\text{probe}} \otimes I_{\text{medium}} + I_{\text{probe}} \otimes H_{\text{medium}} + H_{\text{int}}$$

- Total density matrix

$$\rho_{\text{tot}} = \sum_j p_j |\psi_j\rangle\langle\psi_j| \longrightarrow \frac{d}{dt}\rho_{\text{tot}} = -i[H_{\text{tot}}, \rho_{\text{tot}}]$$

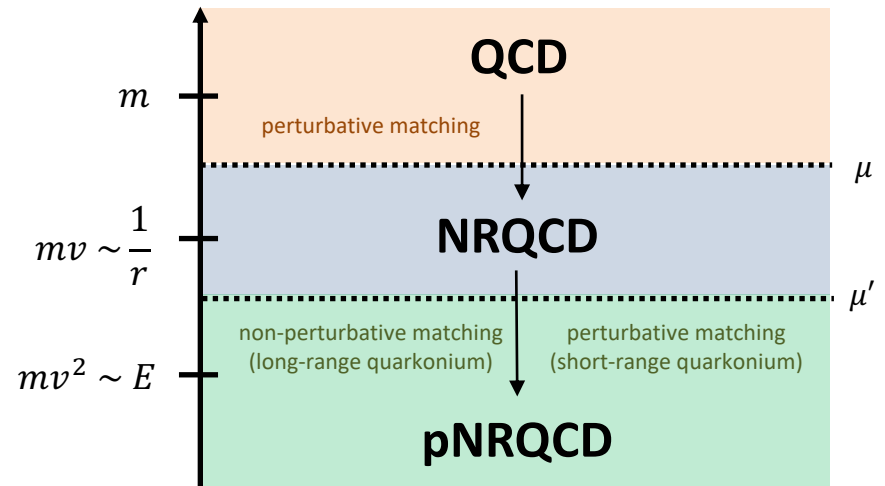
- Reduced density matrix

$$\rho_{\text{probe}} = \text{Tr}_{\text{medium}}[\rho_{\text{tot}}] \longrightarrow \text{“Master equation”}$$

OQS + pNRQCD \rightarrow Lindblad equation

- What are the relevant scales?

- Temperature T
- Bound state mass $m \gg T$
- Bound state size $r \sim 1/mv \sim a_0$ (Bohr radius)
- Debye mass m_D
- Binding energy $E \sim mv^2$



- Separation of time scales

- Medium relaxation time scale $\langle \hat{O}_M(t) \hat{O}_M(0) \rangle \sim e^{-t/t_M} \rightarrow \frac{1}{T}$
- Intrinsic probe time scale $t_P \sim \frac{1}{\omega_i - \omega_j} \rightarrow \frac{1}{E}$
- Probe relaxation time scale $\langle p(t) \rangle \sim e^{-t/t_{\text{rel}}} \rightarrow \frac{1}{\text{self-energy}} \sim \frac{1}{\alpha_s a_0^2 \Lambda^3} \quad \Lambda = T, E$

$$\frac{1/r \gg T \sim m_D \gg E}{t_{\text{rel}}, t_P \gg t_M}$$

$$\frac{d\rho_{\text{probe}}}{dt} = -i[H_{\text{probe}}, \rho_{\text{probe}}] + \sum_n \left(C_n \rho_{\text{probe}} C_n^\dagger - \frac{1}{2} \{C_n^\dagger C_n, \rho_{\text{probe}}\} \right)$$

N. Brambilla, M. A. Escobedo, J. Soto and A. Vairo, 1612.07248, 1711.04515

OQS + pNRQCD – Lindblad reorganization

$$\frac{d\rho_{\text{probe}}}{dt} = -i[H_{\text{probe}}, \rho_{\text{probe}}] + \sum_n \left(C_n \rho_{\text{probe}} C_n^\dagger - \frac{1}{2} \{C_n^\dagger C_n, \rho_{\text{probe}}\} \right)$$

- H_{probe} is Hermitian (includes singlet and octet states)
- C_n are the **collapse (or jump) operators** (connect different internal states)
- Partial and **total decay widths** are

$$\Gamma_n = C_n^\dagger C_n \quad \Gamma = \sum_n \Gamma_n$$

- Can reorganize Lindblad equation by defining

$$H_{\text{eff}} = H_{\text{probe}} - \frac{i}{2} \Gamma$$

← Non-Hermitian effective Hamiltonian

$$\longrightarrow \frac{d\rho_{\text{probe}}}{dt} = -iH_{\text{eff}}\rho_{\text{probe}} + i\rho_{\text{probe}}H_{\text{eff}}^\dagger + \sum_n C_n \rho_{\text{probe}} C_n^\dagger$$

OQS + pNRQCD Hamiltonian and collapse operators

N. Brambilla, M. A. Escobedo, J. Soto and A. Vairo, 1612.07248, 1711.04515

$$\frac{d\rho_{\text{probe}}}{dt} = -iH_{\text{eff}}\rho_{\text{probe}} + i\rho_{\text{probe}}H_{\text{eff}}^\dagger + \sum_n C_n \rho_{\text{probe}} C_n^\dagger$$

$$\rho = \begin{pmatrix} \rho_s & 0 \\ 0 & \rho_o \end{pmatrix}$$

$$H_{\text{probe}} = \begin{pmatrix} h_s & 0 \\ 0 & h_o \end{pmatrix} + \frac{r^2}{2} \gamma \begin{pmatrix} 1 & 0 \\ 0 & \frac{N_c^2 - 2}{2(N_c^2 - 1)} \end{pmatrix}$$

mass shift

$$C_i^0 = \sqrt{\frac{\kappa}{N_c^2 - 1}} r^i \begin{pmatrix} 0 & 1 \\ \sqrt{N_c^2 - 1} & 0 \end{pmatrix},$$

$$C_i^1 = \sqrt{\frac{(N_c^2 - 4)\kappa}{2(N_c^2 - 1)}} r^i \begin{pmatrix} 0 & 0 \\ 0 & 1 \end{pmatrix}.$$

$$\Gamma = \kappa r^i \begin{pmatrix} 1 & 0 \\ 0 & \frac{N_c^2 - 2}{2(N_c^2 - 1)} \end{pmatrix} r^i$$

Total width $\rightarrow \text{Im}[V]$

$$H_{\text{eff}} = H_{\text{probe}} - \frac{i}{2}\Gamma$$

Six collapse operators cover

- singlet \rightarrow octet,
- octet \rightarrow singlet
- octet \rightarrow octet

$$\gamma \equiv \frac{g^2}{6 N_c} \text{Im} \int_{-\infty}^{+\infty} ds \langle T E^{a,i}(s, \mathbf{0}) E^{a,i}(0, \mathbf{0}) \rangle$$

$$\kappa \equiv \frac{g^2}{6 N_c} \text{Re} \int_{-\infty}^{+\infty} ds \langle T E^{a,i}(s, \mathbf{0}) E^{a,i}(0, \mathbf{0}) \rangle$$

OQS + pNRQCD Hamiltonian and collapse operators

N. Brambilla, M. A. Escobedo, J. Soto and A. Vairo, 1612.07248, 1711.04515

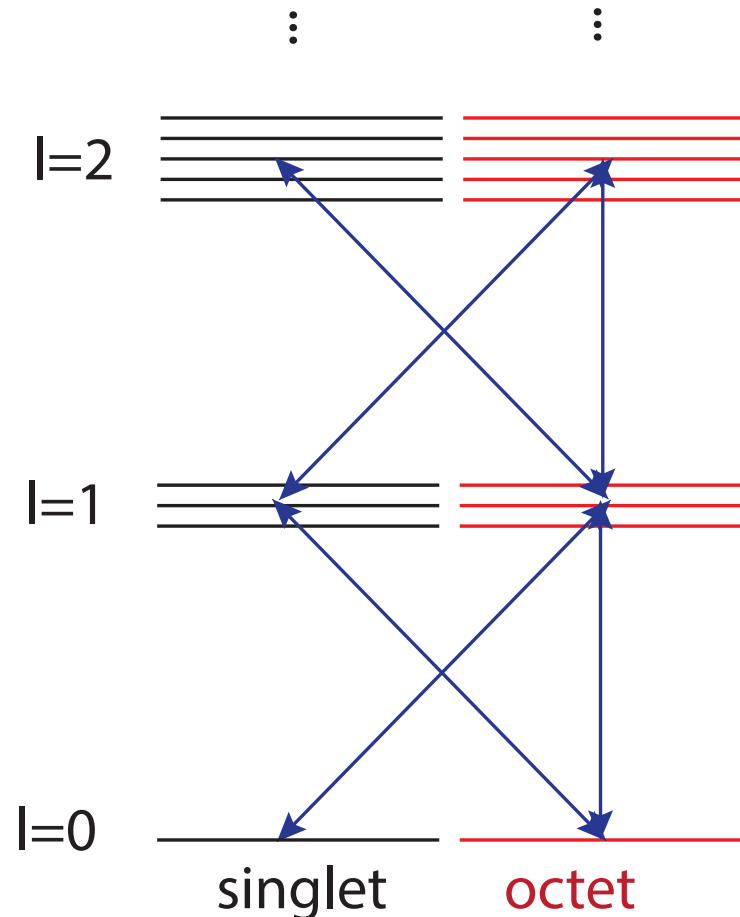
$$\frac{d\rho_{\text{probe}}}{dt} = -iH_{\text{eff}}\rho_{\text{probe}} + i\rho_{\text{probe}}H_{\text{eff}}^\dagger + \sum_n C_n \rho_{\text{probe}} C_n^\dagger$$

$$\rho = \begin{pmatrix} \rho_s & 0 \\ 0 & \rho_o \end{pmatrix}$$

$$C_i^0 = \sqrt{\frac{\kappa}{N_c^2 - 1}} r^i \begin{pmatrix} 0 & 1 \\ \sqrt{N_c^2 - 1} & 0 \end{pmatrix},$$

$$C_i^1 = \sqrt{\frac{(N_c^2 - 4)\kappa}{2(N_c^2 - 1)}} r^i \begin{pmatrix} 0 & 0 \\ 0 & 1 \end{pmatrix}.$$

- Six collapse operators cover**
- singlet \rightarrow octet,
 - octet \rightarrow singlet
 - octet \rightarrow octet



OQS + pNRQCD Hamiltonian and collapse operators

N. Brambilla, M. A. Escobedo, J. Soto and A. Vairo, 1612.07248, 1711.04515

$$\frac{d\rho_{\text{probe}}}{dt} = -iH_{\text{eff}}\rho_{\text{probe}} + i\rho_{\text{probe}}H_{\text{eff}}^\dagger + \sum_n C_n \rho_{\text{probe}} C_n^\dagger$$

$$\rho = \begin{pmatrix} \rho_s & 0 \\ 0 & \rho_o \end{pmatrix}$$

$$H_{\text{probe}} = \begin{pmatrix} h_s & 0 \\ 0 & h_o \end{pmatrix} + \frac{r^2}{2} \gamma \begin{pmatrix} 1 & 0 \\ 0 & \frac{N_c^2 - 2}{2(N_c^2 - 1)} \end{pmatrix}$$

$$C_i^0 = \sqrt{\frac{\kappa}{N_c^2 - 1}} r^i \begin{pmatrix} 0 & 1 \\ \sqrt{N_c^2 - 1} & 0 \end{pmatrix},$$

$$\Gamma = \kappa r^i \begin{pmatrix} 1 & 0 \\ 0 & \frac{N_c^2 - 2}{2(N_c^2 - 1)} \end{pmatrix} r^i$$

$$C_i^1 = \sqrt{\frac{(N_c^2 - 4)\kappa}{2(N_c^2 - 1)}} r^i \begin{pmatrix} 0 & 0 \\ 0 & 1 \end{pmatrix}.$$

Six collapse operators cover

- singlet \rightarrow octet,
- octet \rightarrow singlet
- octet \rightarrow octet

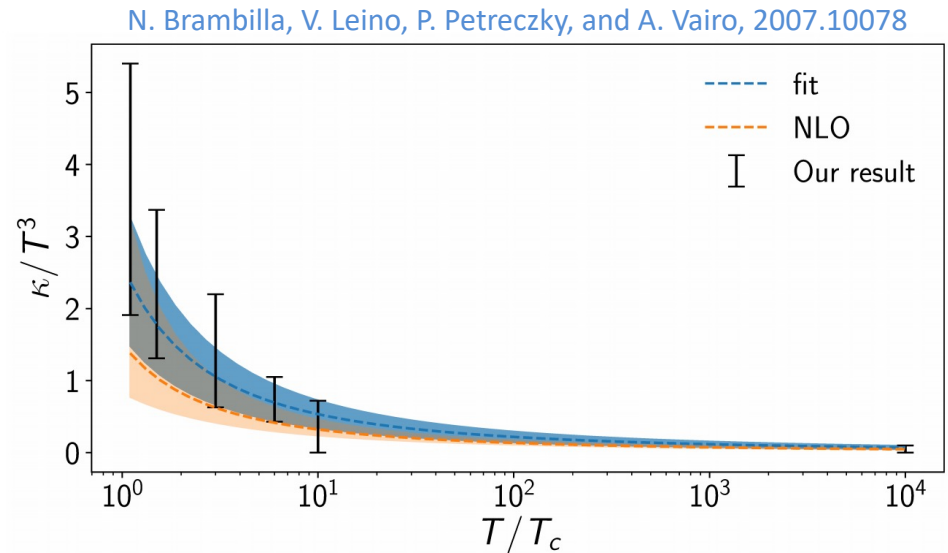
$$\gamma \equiv \frac{g^2}{6 N_c} \text{Im} \int_{-\infty}^{+\infty} ds \langle T E^{a,i}(s, \mathbf{0}) E^{a,i}(0, \mathbf{0}) \rangle$$

$$\kappa \equiv \frac{g^2}{6 N_c} \text{Re} \int_{-\infty}^{+\infty} ds \langle T E^{a,i}(s, \mathbf{0}) E^{a,i}(0, \mathbf{0}) \rangle$$

Values of $\hat{\kappa}$ and $\hat{\gamma}$ used

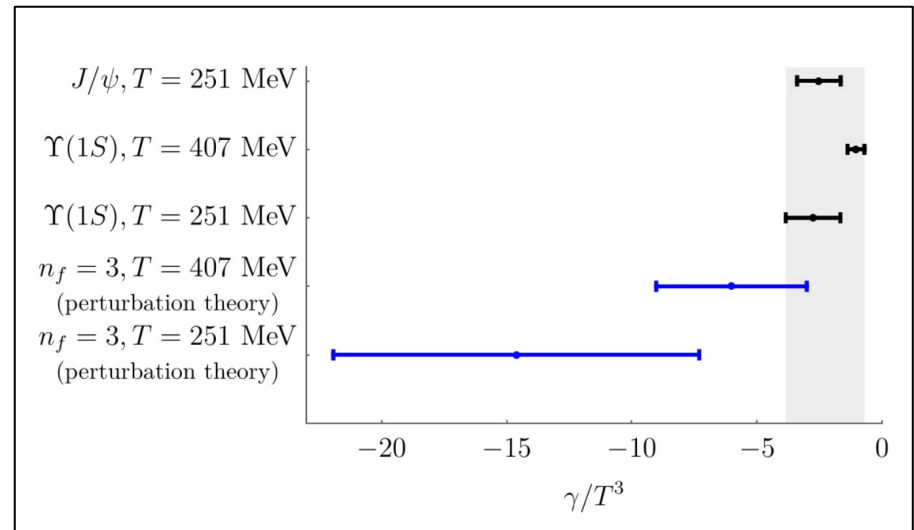
- We used NLO fits to recent lattice measurements of the heavy quark transport coefficient $\hat{\kappa} \equiv \kappa/T^3$. Note that this is related to the heavy quark diffusion constant D .

- N. Brambilla, V. Leino, P. Petreczky, and A. Vairo, 2007.10078



- The value of $\hat{\gamma} \equiv \gamma/T^3$ is less constrained, we vary it in the range $-3.5 < \hat{\gamma} < 0$.

- N. Brambilla, M. A. Escobedo, J. Soto and A. Vairo, 1612.07248.
- N. Brambilla, M. A. Escobedo, J. Soto and A. Vairo, 1711.04515.
- N. Brambilla, M. A. Escobedo, A. Vairo and P. Vander Griend, 1903.08063.



N. Brambilla, M. A. Escobedo, A. Vairo and P. Vander Griend, 1903.08063.

A parallelizable approach: Quantum trajectories

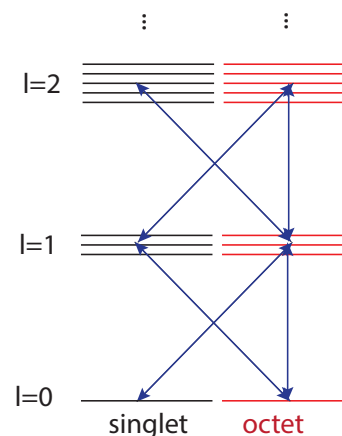
N. Brambilla, M.-A. Escobedo, M.S., A. Vairo, P. Vander Griend, and J.H. Weber, 2012.01240

$$\frac{d\rho_{\text{probe}}}{dt} = -iH_{\text{eff}}\rho_{\text{probe}} + i\rho_{\text{probe}}H_{\text{eff}}^\dagger + \sum_n C_n \rho_{\text{probe}} C_n^\dagger$$

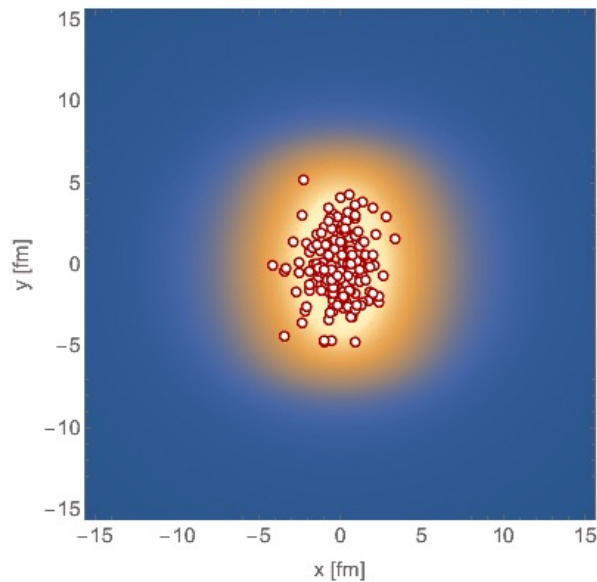
Non-unitary “no jump” evolution

Can treat this “quantum jump” term stochastically

- Can be reduced to the solution of a large set of “quantum trajectories” in which we solve a 1D Schrödinger equation with a **non-Hermitian Hamiltonian H_{eff}** , subject to **stochastic quantum jumps**.
- The evolution with the non-Hermitian H_{eff} preserves the color and angular momentum state of the system (but not norm).
- Collapse/jump operators encode transitions between different color/angular momentum states (subject to selection rules).
- For each **physical trajectory** (path through the QGP) we average over a large set of **independent quantum trajectories** → **Embarrassingly parallel**
- **Added benefit: Can describe all angular momentum states (no cutoff) .**



Computing survival probabilities with QTraj



- We sampled bottomonium production points and initial transverse momentum using **Monte-Carlo sampling** (physical trajectories).
- Temperature evolution provided **by 3+1D anisotropic hydrodynamics** (good description of identified soft hadron spectra and anisotropic flow, see backup slides).
- Along each physical trajectory, we solved the **real-time 3D Schrödinger equation with a complex potential and stochastically sampled jumps** → Lindblad equation.
- We then solved for the **survival probability** of S- and P-wave states (see box to the left).

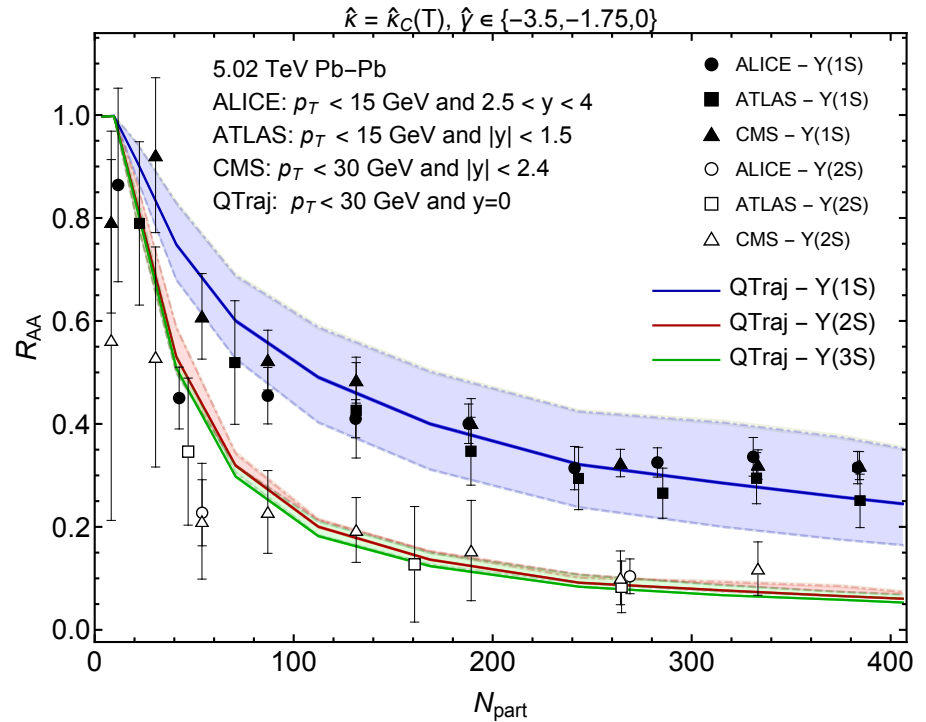
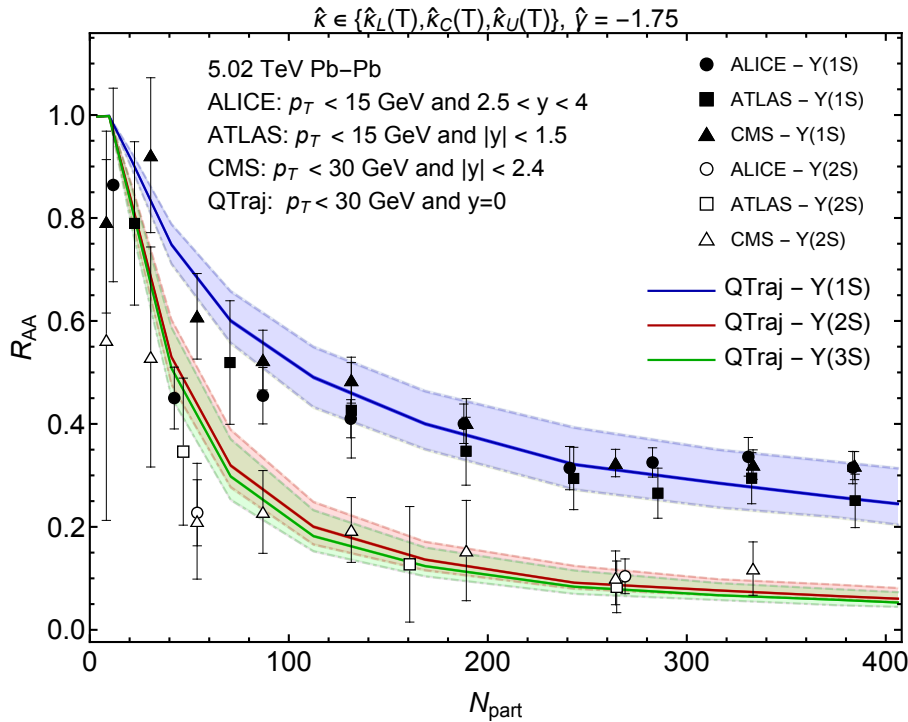
Survival probability

$$SP(n, l) = \frac{|\langle n, l | \psi(t_f) \rangle|^2}{|\langle n, l | \psi(t_0) \rangle|^2}$$

- Used $N = 4096$ points
- $L = 108 a_0$
- $\Delta t = 2 \times 10^{-4}$ fm

OQS + pNRQCD predictions for R_{AA} vs N_{part}

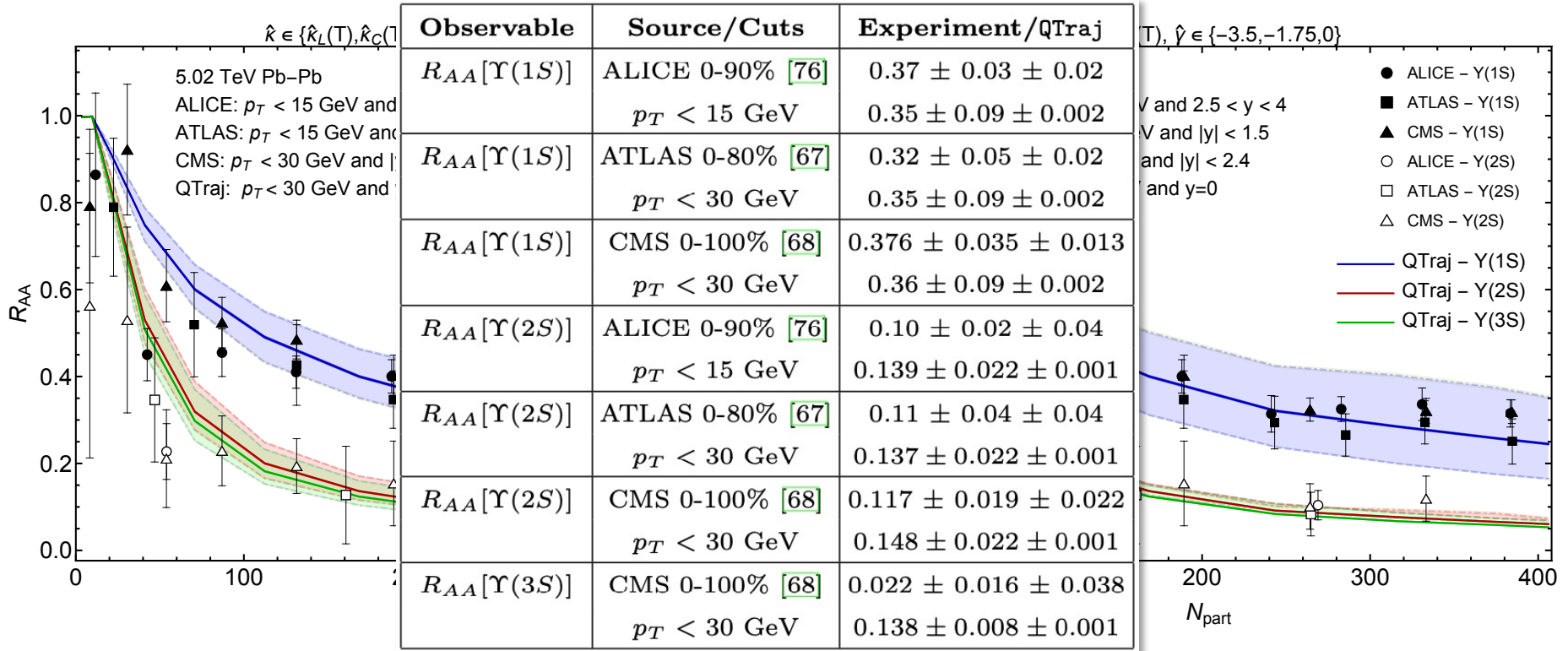
N. Brambilla, M.-A. Escobedo, M.S., A. Vairo, P. Vander Griend, and J.H. Weber, forthcoming



- **Left panel:** Result including feed down, when varying $\hat{\kappa}$ over the theoretical uncertainty.
- **Right panel:** Result including feed down, when varying $\hat{\gamma}$ over the theoretical uncertainty
- Statistical uncertainty associated with average over quantum trajectories is on the order of the line width.

OQS + pNRQCD predictions for R_{AA} vs N_{part}

N. Brambilla, M.-A. Escobedo, M.S., A. Vairo, P. Vander Griend, and J.H. Weber, forthcoming

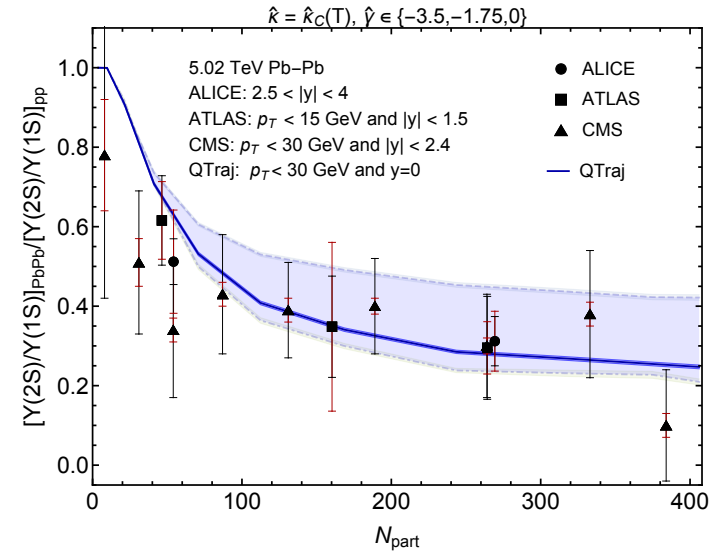
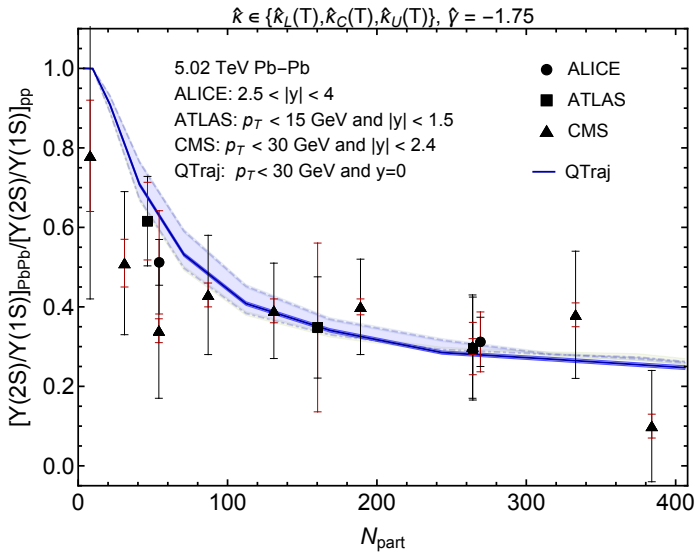


- **Left panel:** Result including feed down, when varying \hat{k} over the theoretical uncertainty.
- **Right panel:** Result including feed down, when varying \hat{y} over the theoretical uncertainty
- Statistical uncertainty associated with average over quantum trajectories is on the order of the line width.

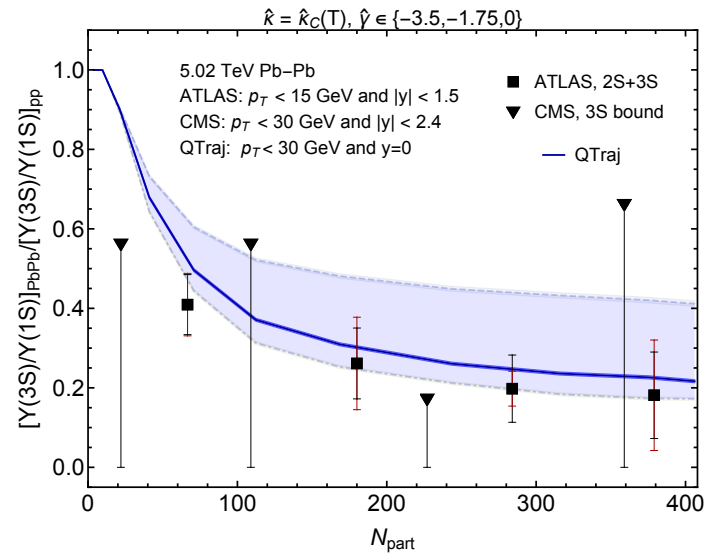
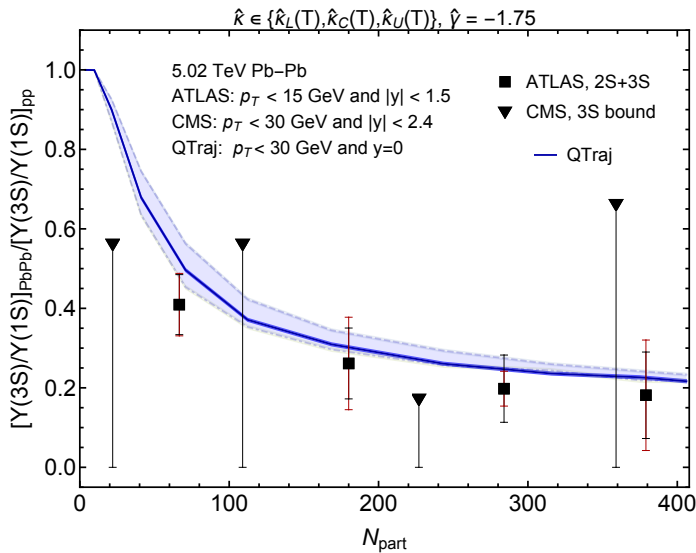
2S/1S and 3S/1S double ratios

N. Brambilla, M.-A. Escobedo, M.S., A. Vairo, P. Vander Griend, and J.H. Weber, forthcoming

2S/1S

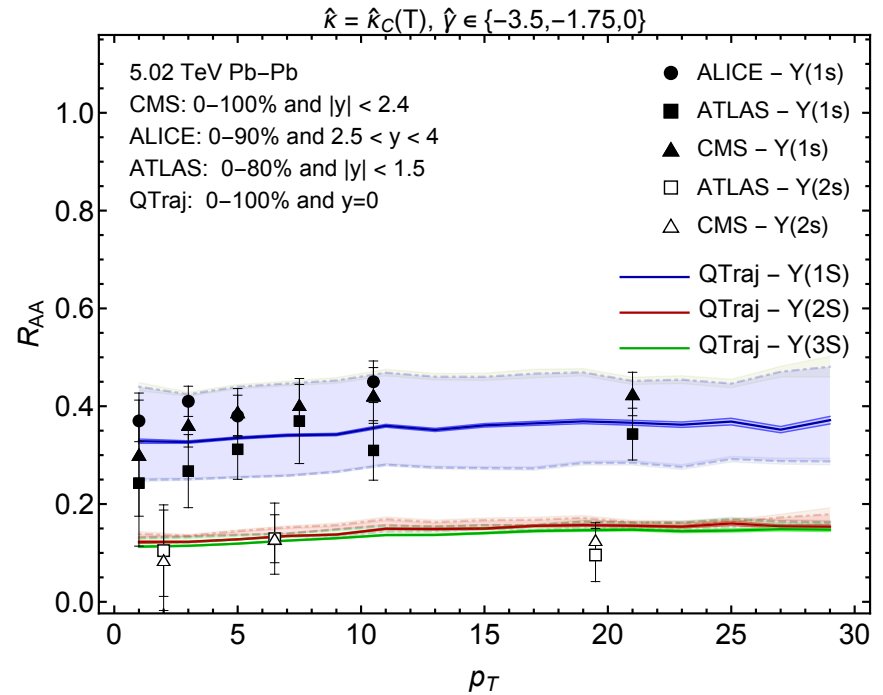
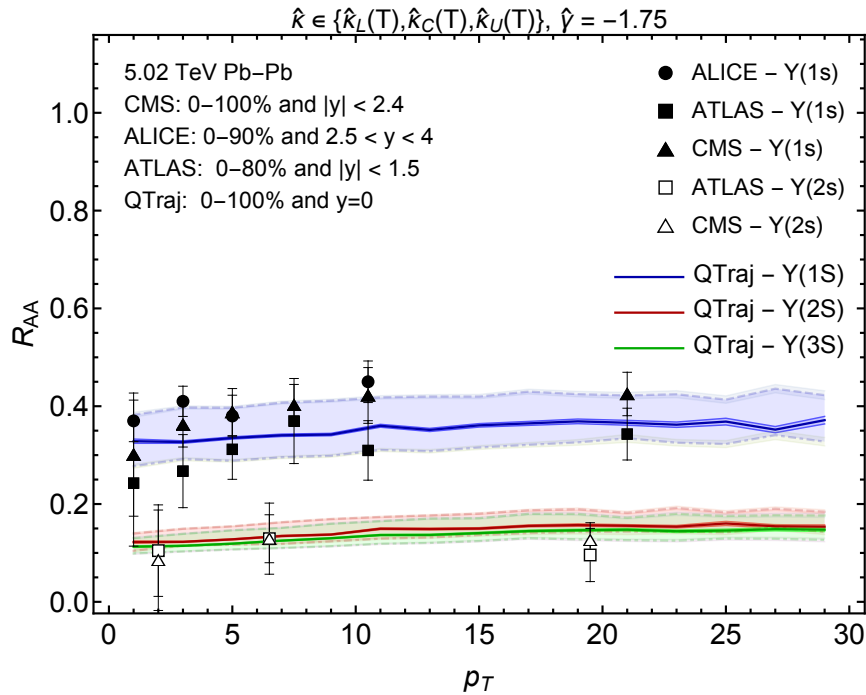


3S/1S



R_{AA} vs transverse momentum

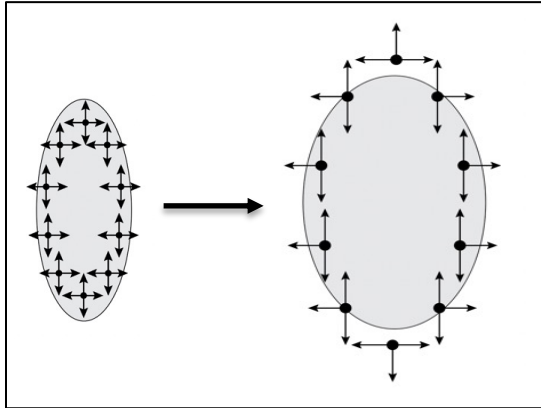
N. Brambilla, M.-A. Escobedo, M.S., A. Vairo, P. Vander Griend, and J.H. Weber, forthcoming



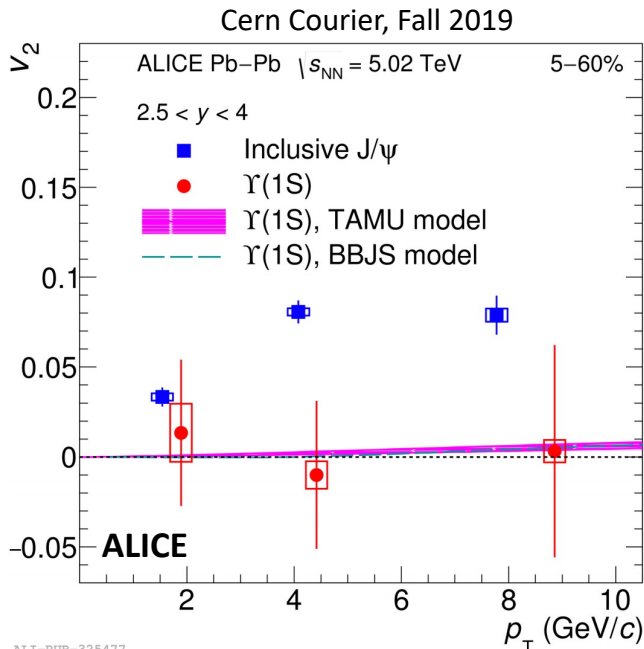
- QTraj predictions consistent with experimental observations.
- Very flat. Small decrease comes from longer time spent in the QGP.
- Once again, larger variation from variation of $\hat{\gamma}$.

Momentum-space anisotropies

4d flow tomography

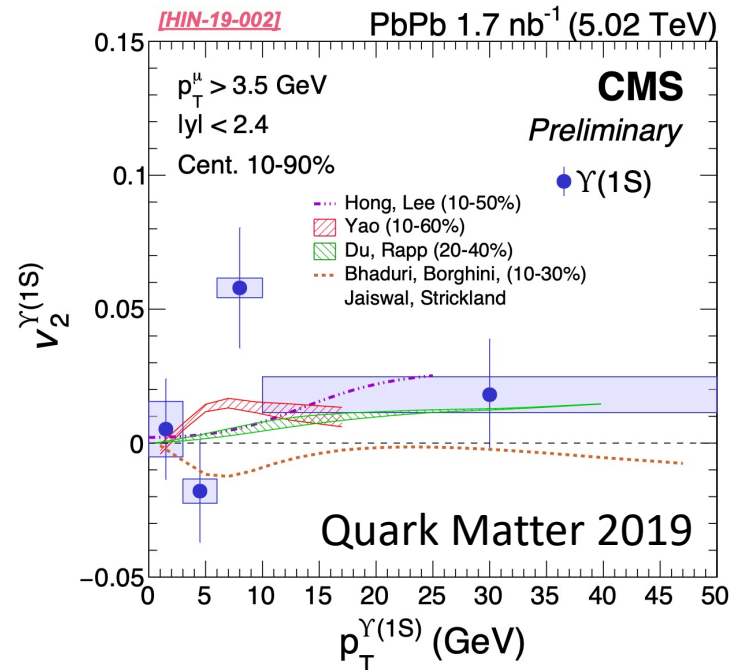


- Bottomonium probably doesn't flow in the "collective flow" sense.
- However, there can be momentum-space anisotropies induced by path-length differences in suppression along the short and long sides of the QGP.



TAMU: Phys. Rev. C 96, (2017) 054901
BJS: arXiv:1809.06235

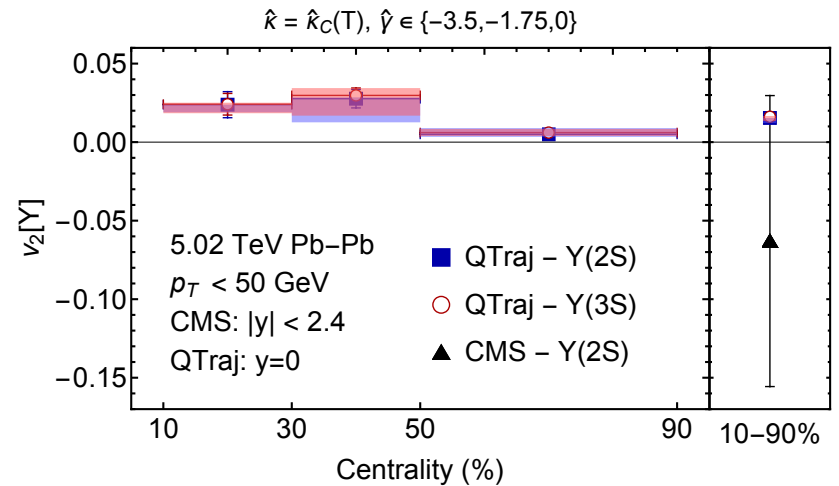
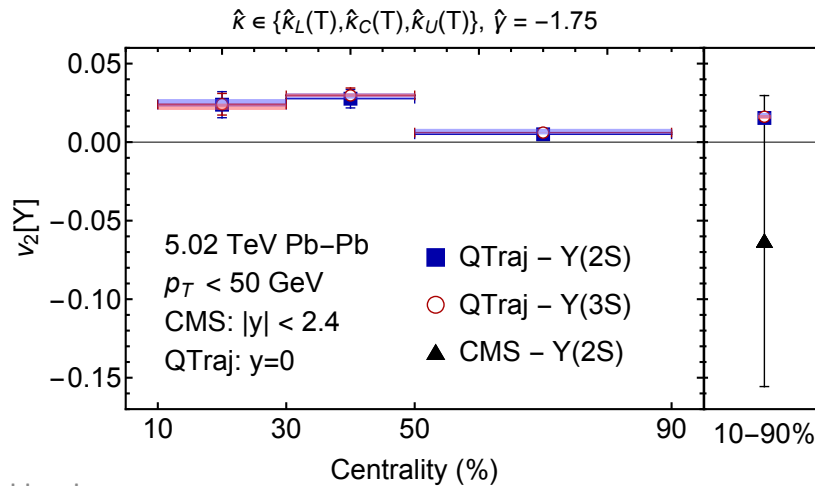
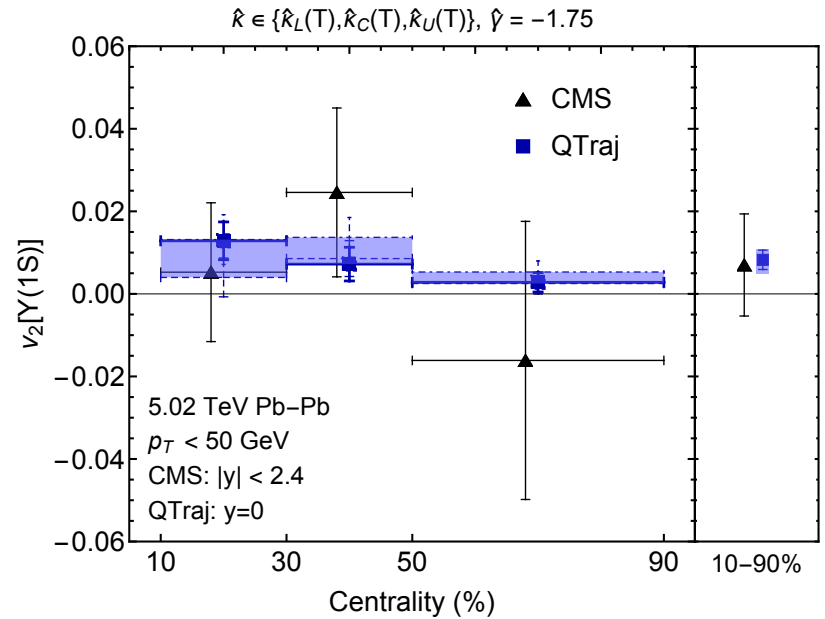
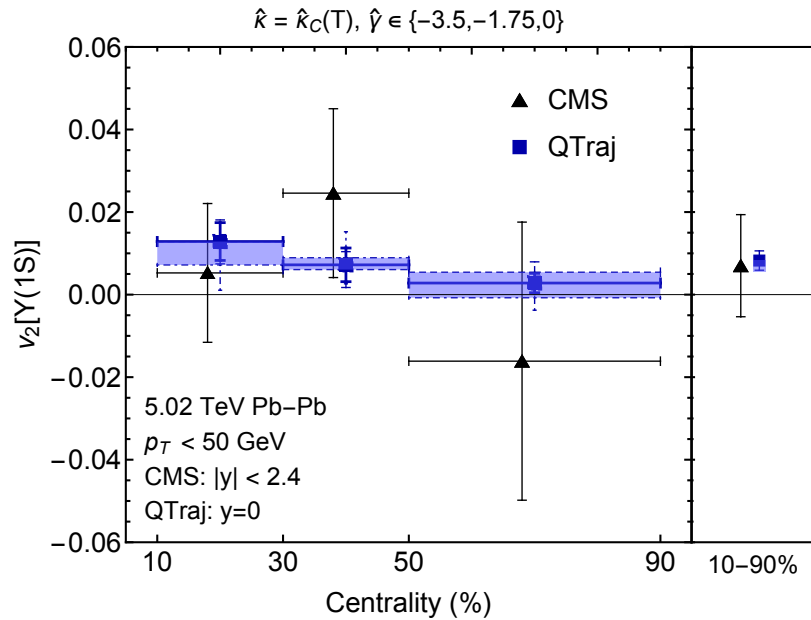
ALICE Collaboration: arXiv:1907.03169



ALI-PUB-325477

Momentum-space anisotropies

N. Brambilla, M.-A. Escobedo, M.S., A. Vairo, P. Vander Griend, and J.H. Weber, forthcoming



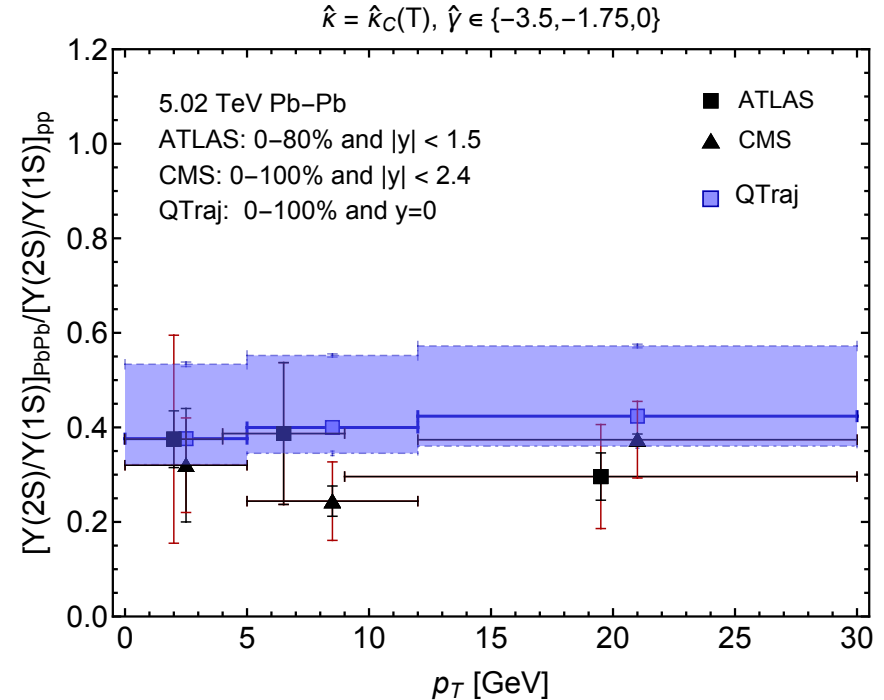
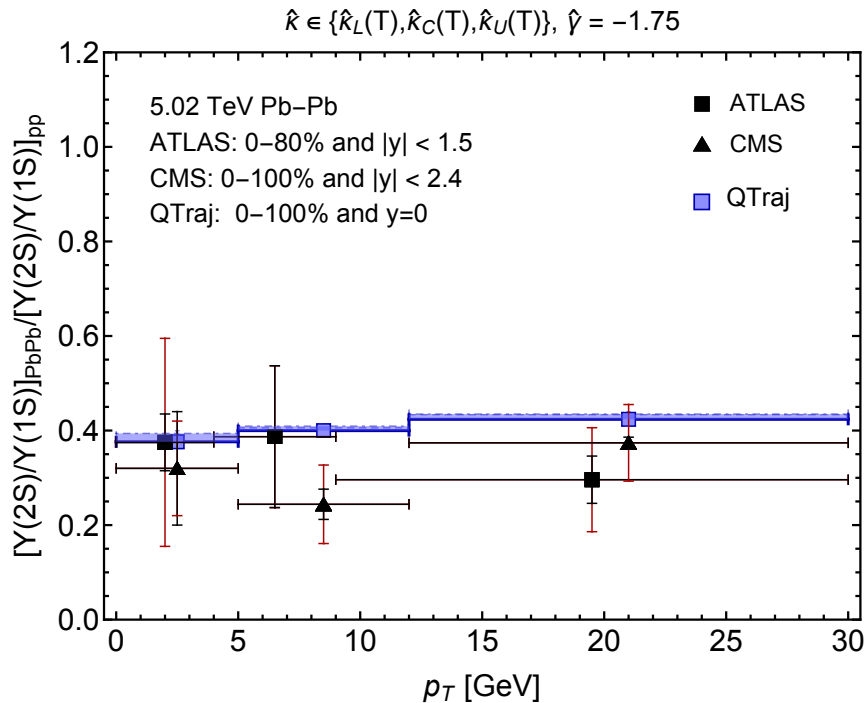
Conclusions and Outlook

- OQS + pNRQCD works very well to describe the suppression vs N_{part} and p_T , double ratios, and “flow” seen at LHC.
- **Full 3D quantum and non-abelian treatment within OQS framework.**
- Transport coefficients used were **constrained by independent lattice measurements.**
- Demonstrated that Upsilon R_{AA} and double ratios can be used to provide **experimental constraints on these transport coefficients.**
- The **quantum trajectory algorithm** (implemented in QTraj) allowed us to include effect of “**quantum jumps**” between color and angular momentum states in a **computationally scalable manner.**
- **QTraj code** has been released along with documentation, see 2107.06147.
- One outstanding issue is the transition to low-temperature bottomonium dynamics ($T < 200 - 250$ MeV). Different ordering of scales, $T \lesssim E \rightarrow$ **work in progress.**

Additional slides

2S/1S ratio vs transverse momentum

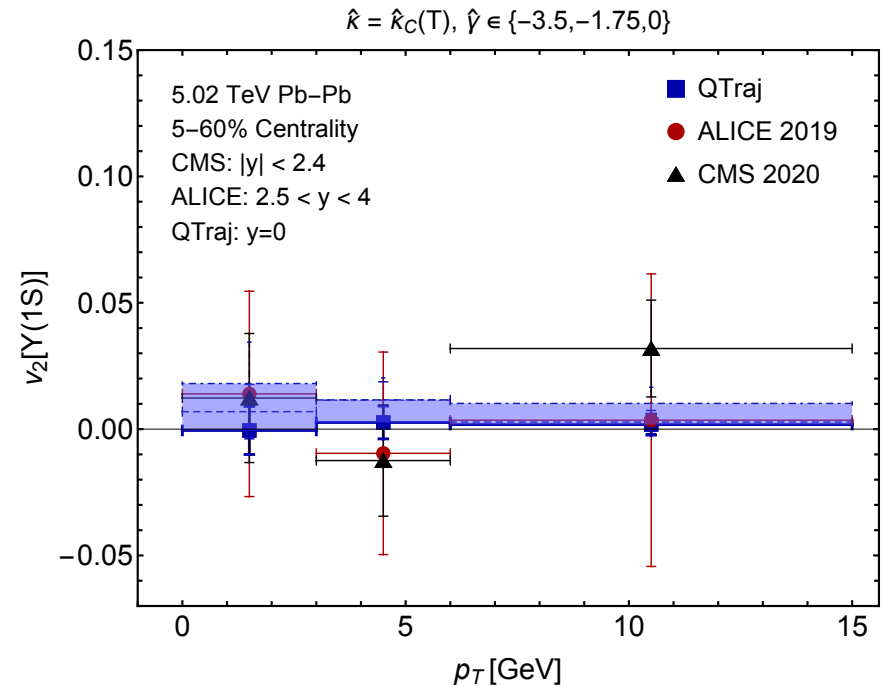
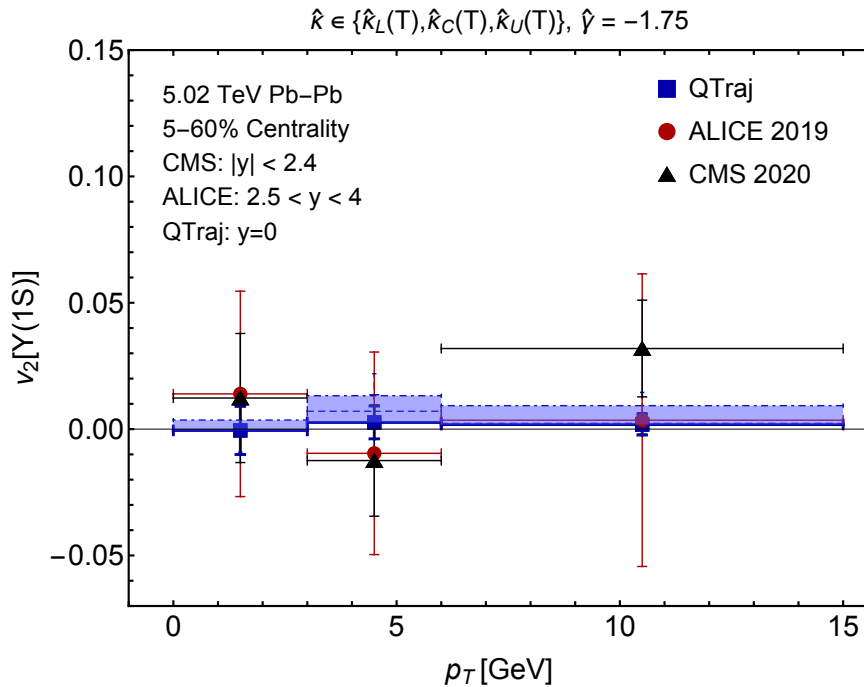
N. Brambilla, M.-A. Escobedo, M.S., A. Vairo, P. Vander Griend, and J.H. Weber, forthcoming



- Result does not depend on choice of κ , however, we see larger variation when varying γ ; **value of $\gamma = -3.5$ has tension with data**
- **This offers some hope to constrain this transport coefficient from 2S/1S double ratio data.**

Momentum-space anisotropies

N. Brambilla, M.-A. Escobedo, M.S., A. Vairo, P. Vander Griend, and J.H. Weber, forthcoming



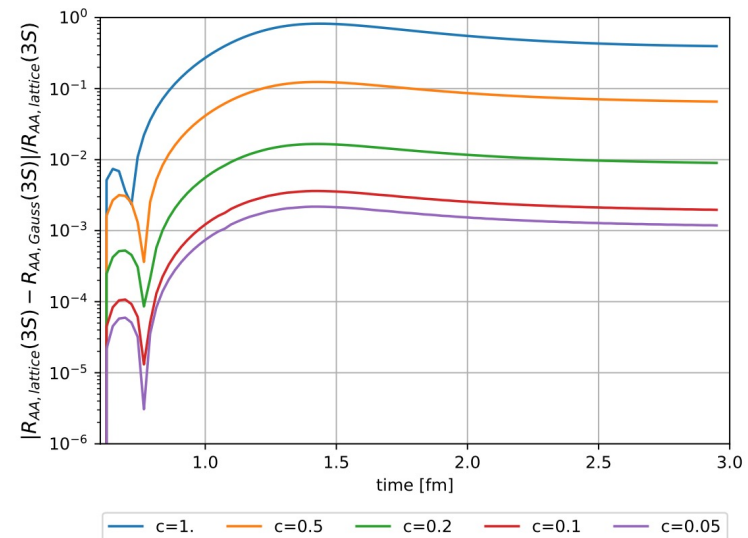
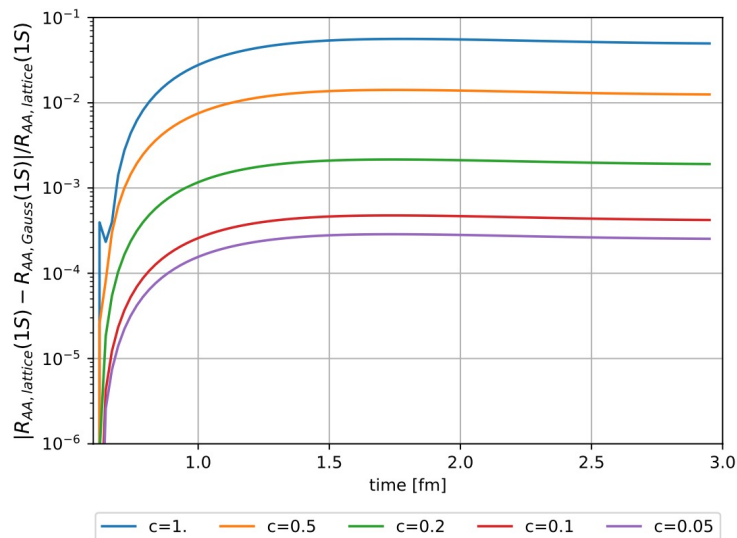
- $Y(1S)$ v_2 due to path length differences in suppression is small.
- **Qtraj predicts $|v_2[Y(1s)]| \lesssim 0.02$ at all p_T .**
- Magnitude is consistent with prior works.
- Data have large uncertainties, hopefully more statistics in the future.

Initial bottomonium wavefunction

- We took the initial wavefunction to be given by a smeared delta function (local production due to large mass, $\Delta \sim 1/M$) of the form

$$u_\ell(r, \tau = 0) \propto r^{\ell+1} \exp(-r^2/\Delta^2)$$

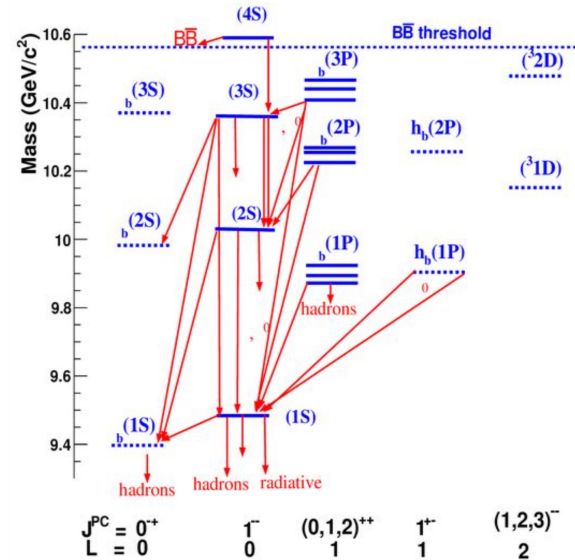
- For a given l , the **initial state is a quantum linear superposition** of the eigenstates of H.
- Includes both bound and unbound states.**
- We took $\Delta = 0.2 a_0$ which reproduces results obtained with a true delta to within 1%.



Feed-down implementation

$$\vec{N}_{\text{observed}} = F \vec{N}_{\text{direct}}$$

$$F = \begin{pmatrix} 1 & 0.2645 & 0.0194 & 0.352 & 0.18 & 0.0657 & 0.0038 & 0.1153 & 0.077 \\ 0 & 1 & 0 & 0 & 0 & 0.106 & 0.0138 & 0.181 & 0.089 \\ 0 & 0 & 1 & 0 & 0 & 0 & 0 & 0 & 0 \\ 0 & 0 & 0 & 1 & 0 & 0 & 0 & 0.0091 & 0 \\ 0 & 0 & 0 & 0 & 1 & 0 & 0 & 0 & 0.0051 \\ 0 & 0 & 0 & 0 & 0 & 1 & 0 & 0 & 0 \\ 0 & 0 & 0 & 0 & 0 & 0 & 1 & 0 & 0 \\ 0 & 0 & 0 & 0 & 0 & 0 & 0 & 1 & 0 \\ 0 & 0 & 0 & 0 & 0 & 0 & 0 & 0 & 1 \end{pmatrix}$$



- N_{direct} corresponds to $(N_{1S}, N_{2S}, N_{1P} \times 3, N_{3S}, N_{2P} \times 3, N_{2D})^T$ where, e.g., N_{1S} is the final number of $Y(1S)$ states that can decay in the dilepton channel.
- N_{direct} can be obtained using $\langle N_{\text{bin}}(b) \rangle * \sigma_{\text{direct}} * (\text{Survival probability})$
- After feed down, we then normalize to by the pp collision result scaled to AA $\rightarrow R_{AA}$.

$$R_{AA}^i(c) = \frac{(F \cdot S(c) \cdot \vec{\sigma}_{\text{direct}})^i}{\sigma_{\text{exp}}^i}$$

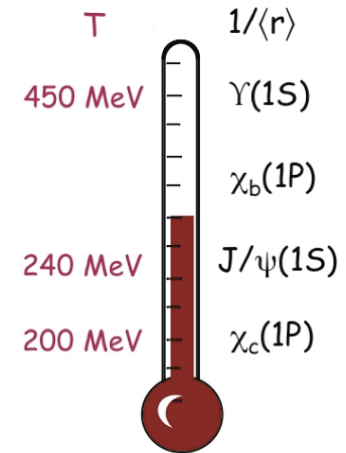
How can one numerically solve these equations?

$$\frac{d\rho_{\text{probe}}}{dt} = -iH_{\text{eff}}\rho_{\text{probe}} + i\rho_{\text{probe}}H_{\text{eff}}^\dagger + \sum_n C_n \rho_{\text{probe}} C_n^\dagger$$

- Each block of the density matrix in color space can be decomposed into orbital angular momentum blockwise.
- Upon truncating in angular momentum ($l \leq l_{\text{max}}$) one can reduce both the singlet and octet blocks of the reduced density matrix to size $(l_{\text{max}} + 1)^2$.
- One can then discretize the radial wavefunction ($N = \#$ of lattice points) and evolve the reduced density matrix using standard differential equation and matrix solvers gives $\sim N^2(l_{\text{max}} + 1)^2$ matrix size.
- **Need to describe bound and unbound states with highly localized initial wave function, so the box must be large and have small lattice spacing \rightarrow large N and large l_{max} .**
- As N and l_{max} become large, the computation becomes very challenging.
- **Need a better/faster method which we can easily parallelize.**

Bottomonia are excellent probes of the QGP

- Can trust heavy quark effective theory more.
- Cold nuclear matter (CNM) effects in AA decrease with increasing quark mass.
- The masses of bottomonia ($m \sim 10 \text{ GeV}$) are much higher than the temperature generated in HICs ($T < 1 \text{ GeV}$) \rightarrow bottomonium production dominated by initial hard scatterings.
- Both closed and open bottom production is quite rare in RHIC and LHC energy HICs \rightarrow the probability for regeneration of bottomonia through statistical recombination is much smaller than for charm quarks; less model uncertainty.

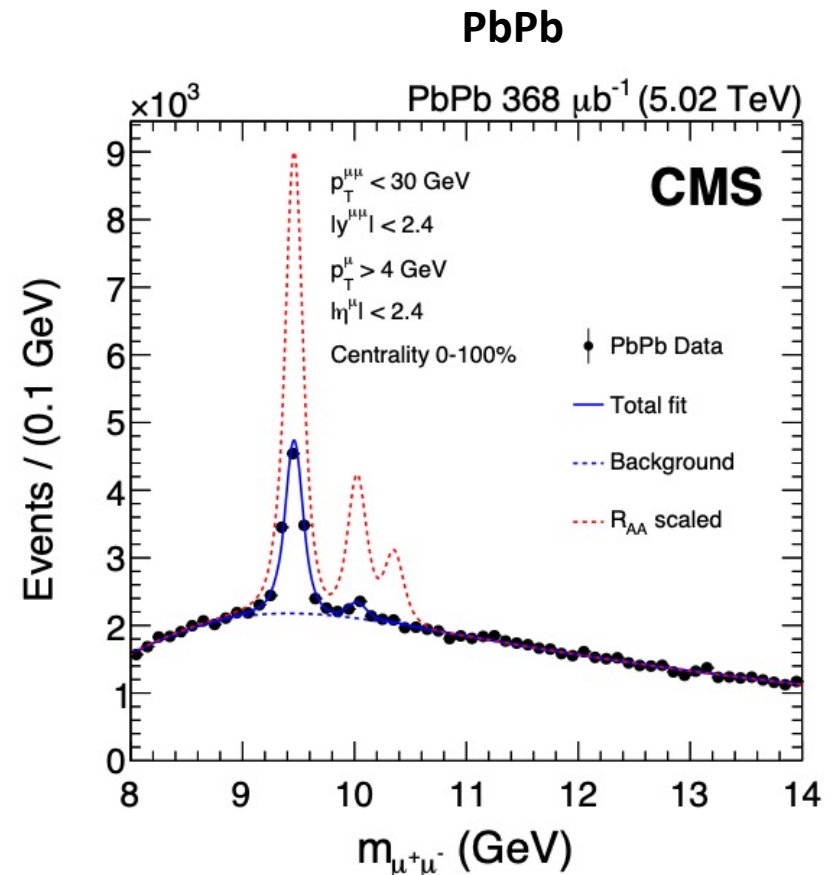
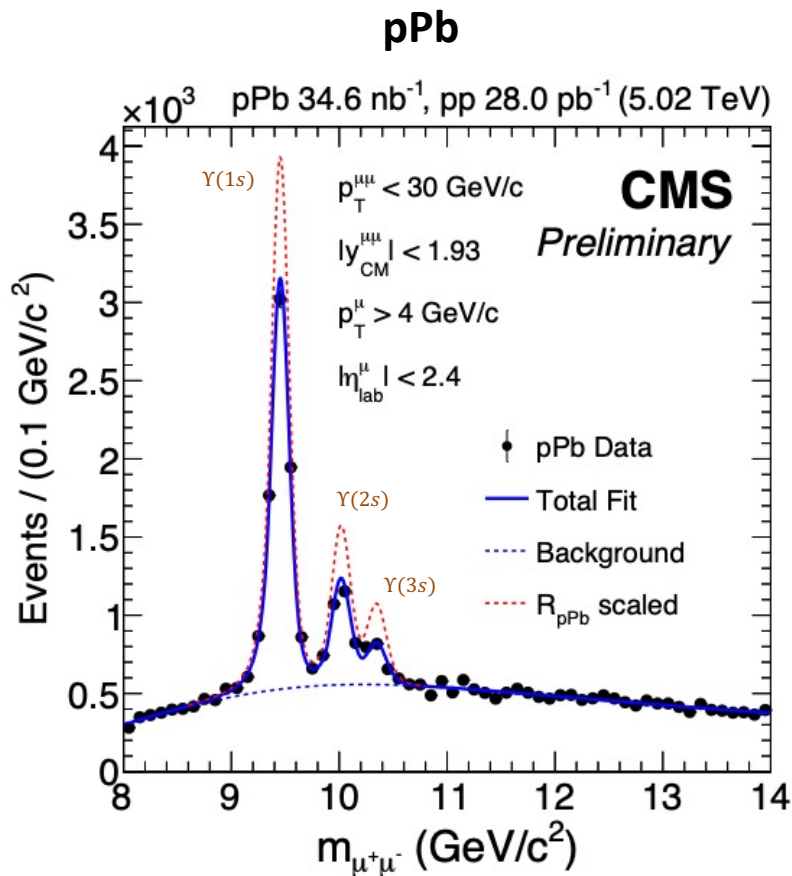


A. Mocsy, P. Petreczky,
and MS, 1302.2180

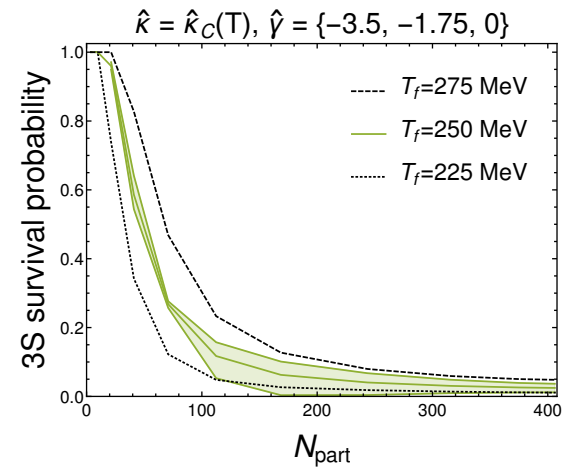
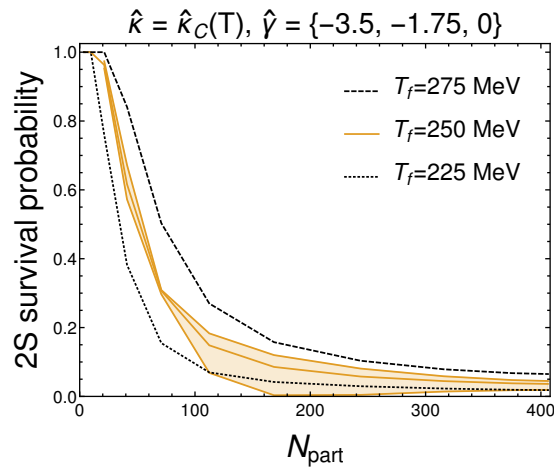
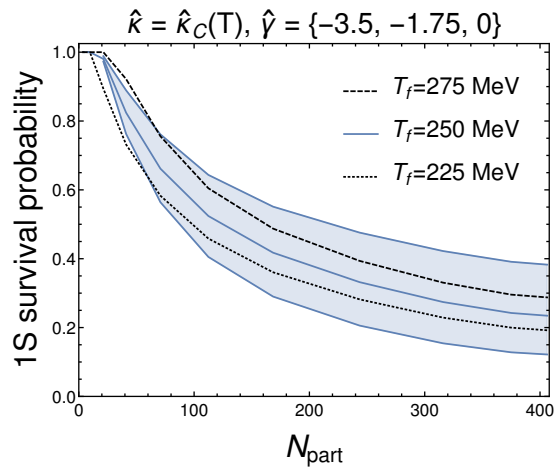
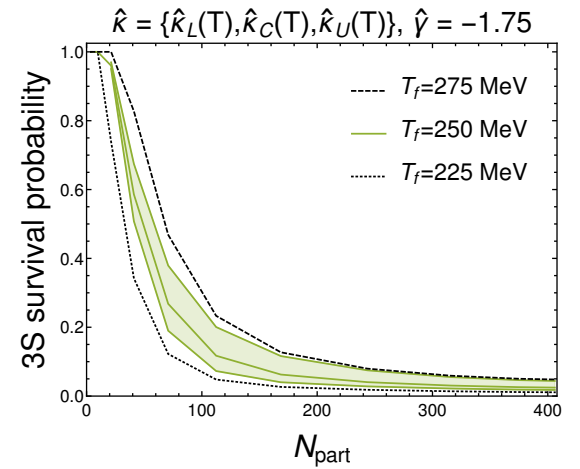
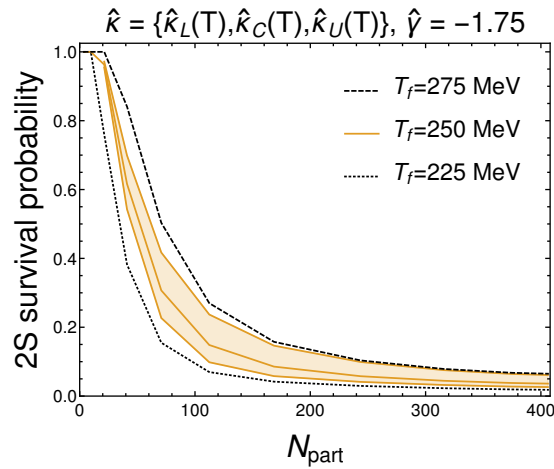
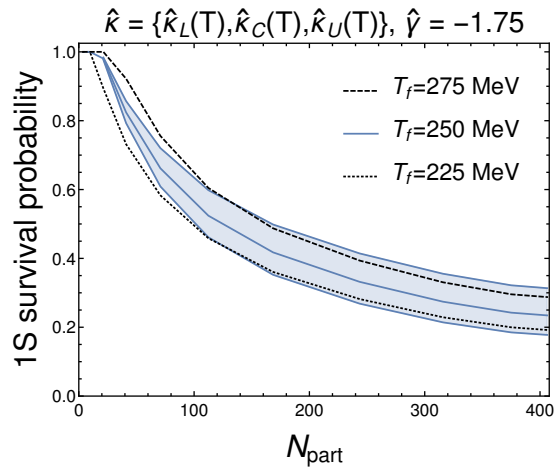
[see e.g. E. Emerick, X. Zhao, and R. Rapp, arXiv:1111.6537 and others]

Experimental data – 5.02 TeV Dimuon Spectra

The **CMS**, **ALICE**, and **ATLAS** experiments have measured bottomonium production in both pp and Pb-Pb collisions. Here I show CMS results.

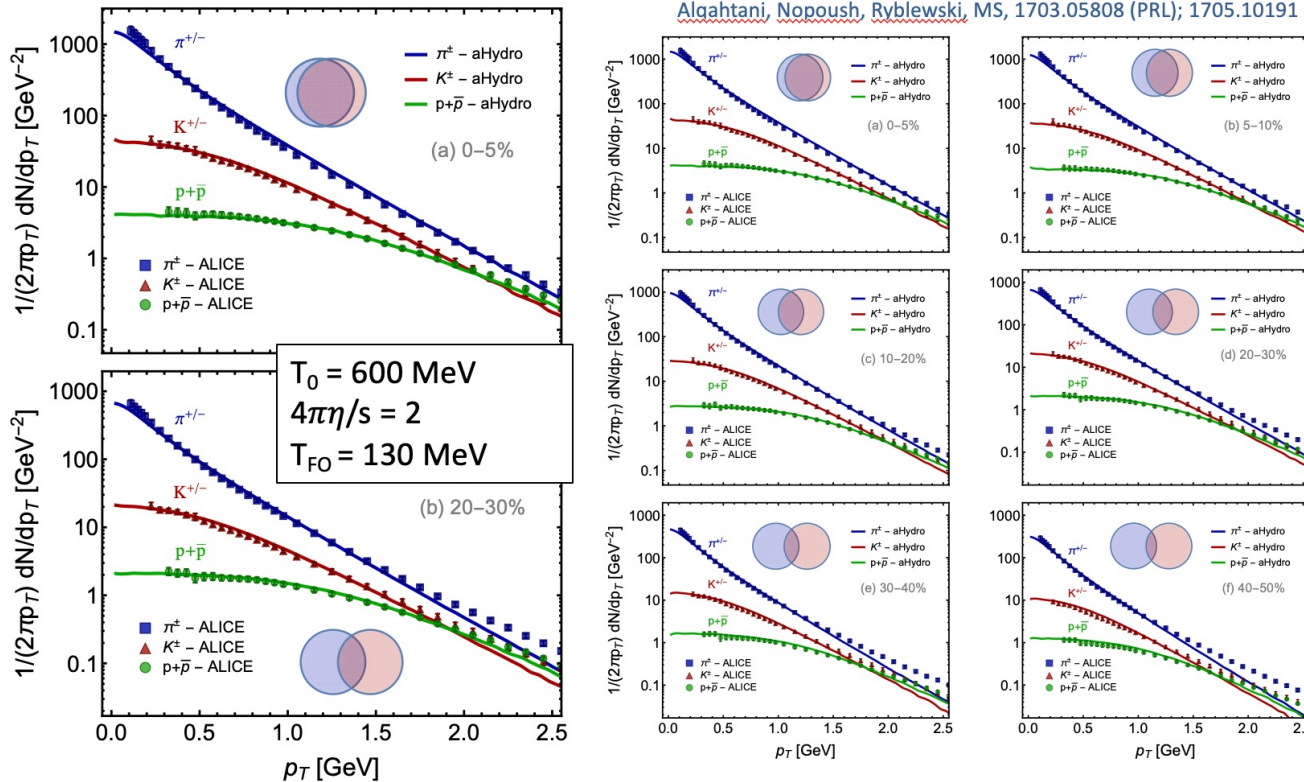


Dependence on T_f



3+1D hydrodynamical background

Identified particle spectra



M. Strickland

Data are from the ALICE collaboration data for **Pb-Pb collisions @ 2.76 TeV/nucleon**

6

- We use a 3+1D dissipative code for the hydro background (quasiparticle anisotropic hydrodynamics)
- Has been tuned to RHIC and LHC heavy ion collisions
- Reproduces spectra, multiplicities, identified elliptic flow of light hadrons, HBT radii, etc.

For 5.02 TeV, $T_0 = 630 \text{ MeV}$ @ $t_0 = 0.25 \text{ fm}/c$